A FLEXIBLE SYSTEM FOR ESTIMATION OF INFILTRATION AND HYDRAULIC RESISTANCE PARAMETERS IN SURFACE IRRIGATION

E. Bautista, J. L. Schlegel

ABSTRACT. *Characterizing the infiltration and hydraulic resistance process is critical to the use of modeling tools for the hydraulic analysis of surface irrigation systems. Because those processes are still not well understood, various formulations are currently used to represent them. A software component has been developed for estimation of the parameters of infiltration and hydraulic resistance models. Infiltration computations rely on volume balance analysis. The software provides flexibility for defining the estimation problem with various data configurations. The procedure works with various infiltration and resistance formulations. Given the inherent inaccuracies of volume balance analysis, the software provides tools for identifying and correcting some of those inaccuracies. Computational tests are provided to illustrate the capabilities and limitations of the proposed procedures.*

Keywords. *Basin irrigation, Border irrigation, Computer model, Computer software, Furrow irrigation, Model calibration, Surface irrigation, Water management, WinSRFR.*

WinSRFR is a software package for the hydraulic analysis of irrigation systems that offers simulation, event analysis, design, and operational analysis functionalities (Bautista et al., 2009a). The event analysis component is used to estimate infiltration parameters and evaluate the performance of irrigation systems from field-measured data. Currently, the software offers two estimation procedures, a modified version of the post-irrigation volume balance method (PIVB) (Merriam and Keller, 1978), and the two-point method (Elliott and Walker, 1982), each with its own specific data requirements. These options are limited considering the various combinations of data that can be collected during an irrigation evaluation. An additional limitation is that these procedures cannot be use to estimate parameters for all infiltration models offered by WinSRFR or to estimate the hydraulic resistance parameter. Hence, a new estimation option has been developed and will be made available with WinSRFR 5. This article describes that component.

Submitted for review in September 2016 as manuscript number NRES 12117; approved for publication by the Natural Resources & Environmental Systems Community of ASABE in March 2017.

Mention of company or trade names is for description only and does not imply endorsement by the USDA. The USDA is an equal opportunity provider and employer.

The authors are **Eduardo Bautista, ASABE Member,** Research Hydraulic Engineer, and **James L. Schlegel,** Software Developer, USDA-ARS U.S. Arid Land Agricultural Research Center, Maricopa, Arizona. **Corresponding author:** Eduardo Bautista, U.S. Arid Land Agricultural Research Center, 21881 North Cardon Lane, Maricopa, AZ 85138; phone: 520-316-6381; e-mail: Eduardo.Bautista@ars.usda.gov.

OBJECTIVES AND DESCRIPTION

The primary objective of this development is to provide greater flexibility in formulating a parameter estimation problem and therefore in defining a field evaluation strategy. The evaluation strategy defines the irrigation outputs measured in the field, which are limited to surface flow variables: advance times, recession times, flow depths with distance and time, and runoff rate in the case of free-draining systems. For routine applications, these measurements can be costly and/or difficult to obtain. Hence, methods that use limited measurements, such as the two-point method, are relatively popular. However, numerous studies have shown that the reliability of estimation results depends on the type and quality of data provided and whether those data represent the entire irrigation event or only a portion of it (e.g., Katopodes, 1990; Gillies and Smith, 2005; Walker, 2005). It should be clear then that any estimation or evaluation strategy needs to consider the tradeoffs between the minimum data needed to properly evaluate the infiltration and hydraulic resistance characteristics of an irrigation system under the particular field conditions, and the costs of obtaining such information. A flexible estimation approach may encourage users to focus their measurement effort on irrigation outputs that provide the most information about the processes of interest.

The development of micro-electronic sensors will make the problem of collecting essential data less challenging and costly in the near future. Thus, the expectation is that the collection of more data, in particular flow depth hydrographs, will become more common and that software applications that can handle those data will be required. At the same time, field evaluations will not always produce all of the desired data. Measurement devices, e.g., flumes for measurement of runoff, may be difficult to install under

particular field conditions, or equipment may be damaged or lost in the field. Considering those possibilities, the estimation strategy needs to be adaptable and make the best use of the available data.

A second objective is to expand the selection of infiltration models that can be used in parameter estimation. Parameter estimation procedures in WinSRFR 4 apply only to empirical models, where infiltration is assumed dependent on opportunity time only, and not all of the empirical infiltration modeling options offered by the software are supported. Those procedures do not support the estimation of parameters for models in which infiltration depends on the time and space variable flow depth, such as the Green-Ampt model (Green and Ampt, 1911). The new estimation component supports these flow-depth dependent infiltration formulations and the estimation of hydraulic resistance.

Estimation methods based on volume balance have inherent inaccuracies that users often fail to understand. Those inaccuracies can lead to poor results. The alternative is to solve the estimation problem using unsteady flow equations in combination with optimization techniques. In principle, these methods require less effort by the user. However, they are computationally intensive, can fail to converge or converge to a non-optimal solution and, in those cases, provide few options to the user to adjust the analysis. With proper feedback and guidance, volume balance techniques can always yield a reasonable solution. Hence, a final objective of this development is provide mechanisms for improving the volume balance analysis, and ultimately improving the reliability of results.

The new system provides a consolidated volume-balance based estimation option, compatible with the data sets used by the PIVB and two-point options. The system is supported by unsteady flow simulation, which is used to test the estimates derived from volume balance and guide the needed adjustments to those estimates. Because the development of the system began as an effort to incorporate the EVALUE estimation methodology (Strelkoff et al., 1999) into WinSRFR and enhance that approach, the new estimation component is identified as the EVALUE option in WinSRFR 5.

ESTIMATION OF INFILTRATION PARAMETERS BY VOLUME BALANCE

Volume balance analysis determines the infiltrated volume V_z [L^3] at selected times t_i as the residual of the inflow, surface, and runoff volumes (V_{in}, V_y, and V_{ro}, respectively), each with dimensions [L^3]:

$$V_z(t_i) = V_{in}(t_i) - V_y(t_i) - V_{ro}(t_i) \tag{1}$$

The parameters α_1, α_2, ... α_n of the selected infiltration model are found by matching this residual, calculated at one or more times, with predicted values V_z^* found by integrating the infiltration profile:

$$V_z^*(t_i) = \int_0^{x_A(t_i)} A_z[y(x,t), \alpha_1, \alpha_2, \ldots, \alpha_n]dx \tag{2}$$

The upper bound of the integral is the stream length (i.e., the advance distance) x_A [L], where $x_A \le L_f$, the field length [L]. In the general case, A_z [L^3/L] is a function of the time and space dependent flow depths, but volume balance analyses typically assume that it is a function only of intake opportunity time, as will be discussed later. In general, the volume balance estimation problem can then be described as the problem of minimizing the sums-of-squares objective function:

$$OF = \sum_{i=1}^{I} \left(V_z - V_z^*\right)^2 \tag{3}$$

The times t_i at which both equations 1 and 2 can be applied depend on the available data and hydraulic considerations. Hence, volume balance calculation times are determined by the software using a set of rules. Those rules also prevent the analysis from executing if the data present inconsistencies or do not meet certain requirements. In those cases, the user still has the option to use those data for validation purposes, but they have to be excluded from the volume balance analysis. As an example, an evaluation may yield a set of flow depth measurements that may be insufficient for surface volume calculations but that still may be adequate for examining hydraulic resistance. The user then has to state that flow depth data are available but will not be used for volume balance calculations.

SURFACE VOLUMES

A key difficulty in volume balance analyses is determining the surface volume. Typically, those calculations use hydraulic relationships to estimate the depth profile as a function of distance. Integration of the depth profile yields V_y. Alternatively, the depth profile can be determined from measured surface depth hydrographs. Details are provided next.

Estimated Surface Volumes

Surface volumes are estimated as:

$$V_y = A_{y0}\sigma_y x_A \tag{4}$$

where A_{y0} [L^2] is the upstream flow area, which is a function of the upstream flow depth y_0 [L], σ_y a shape factor [.], and x_A was previously defined. A typical approach for solving equation 4 is by letting $y_0 = y_n$, the normal depth calculated at the average inflow rate, and $\sigma_y = 0.77$, but this can lead to large estimation errors under a wide range of conditions (Bautista et al., 2012a). The EVALUE component uses a combination of analytical procedures and simulation results to compute V_y.

Valiantzas (1993) proposed procedures for calculating y_0 and σ_y by assuming that the flow depth profile $y(x)$ follows a power law:

$$y(x) = y_0\left(1 - x/x_A\right)^{\beta} \tag{5}$$

where y_0 is the upstream depth at time t_i, and β [.] is an empirical parameter, which is discussed later. An implicit expression for y_0 can be derived by combining equation 5 with a hydraulic resistance equation. When using the Manning (1889) formula, the resulting expression is:

$$\beta \frac{y_0}{x_A} = S_0 - \left(\frac{Q_{in} n}{c_u A_{y0} R_0^{2/3}} \right)^2 \quad (6)$$

where c_u is a unit conversion coefficient (= 1.0 in SI units), R_0 is the hydraulic radius [L], which like A_{y0} depends on y_0, and n [$L^{1/6}$] is the Manning roughness coefficient. With this expression, y_0 varies with time as a function of x_A and Q_{in}. Gillies et al. (2007) previously discussed inaccuracies of the volume balance method when inflow rate variations are not accounted for.

With y_0 known, V_y can be calculated by combining equation 5 with an expression for the cross-sectional geometry of the channel and integrating over the stream length:

$$V_y = \int_0^{x_A} A_y[y(x)]dx \quad (7)$$

Equation 7 can then be combined with equation 4 to find σ_y for specific channel geometries. In the case of a trapezoidal furrow with bottom width B_0 and side slopes SS, σ_y is given by:

$$\sigma_y = \frac{1}{A_0} \left(\frac{y_0 B_0}{\beta + 1} + \frac{y_0^2 SS}{2\beta + 1} \right) \quad (8)$$

For a parabolic furrow, the top width as a function of depth is given by:

$$T = cy^m \quad (9)$$

$$\sigma_y = \frac{1}{\beta(m+1)+1} \quad (10)$$

In equation 9, c [L^m] and m [.] are empirical parameters. For borders, the result is simply:

$$\sigma_y = \frac{1}{\beta + 1} \quad (11)$$

These calculations apply only when $Q_{in} > 0$, and they need to be modified after the stream has reached the end of the field in free-draining systems (Bautista et al., 2012a). They are inapplicable for post-advance calculations in blocked-end systems, due to backwater effects.

Complicating the use of equations 6, 8, 10, and 11 is that β is not known *a priori* and depends on the unknown infiltration conditions (in addition to stream length, bottom slope, and cross-section) (Bautista et al., 2012a). Under some field conditions, β can be nearly constant (about 0.45); under other conditions, it can vary substantially (as much as 0.1 to 0.6). This problem is resolved by calculating y_0 and σ_y with the help of unsteady simulation results (Bautista et al., 2012a). The analysis begins with an initial guess for β, provided by the software, resulting in an initial set of infiltration parameters. Inadequate estimates for β will result in noticeable volume balance errors EV_y, defined as:

$$EV_y(t_i) = \frac{V_y(t_i) - V_y^{sim}(t_i)}{V_{in}(t_i)} \times 100 \quad (12)$$

and consequently disagreements between observations and simulation results. In the previous expression, the superscript *sim* refers to a simulated value. The application computes and displays these errors when verifying the estimated solution. New estimates for β can be extracted from the unsteady simulation results, which can then be used to calculate new volume estimates, and therefore a new infiltration solution. The refinement procedure is handled by the software. Generally, one iteration of this process is needed, as estimates of β are most sensitive to stream length and slope, which are constants for a particular problem.

A bigger challenge with the above-described calculations is that equation 6 depends on the hydraulic resistance parameter that, typically, we are also trying to estimate. The NRCS (USDA-SCS, 1984) has recommended values for the roughness coefficient of the Manning equation, which is widely used to model hydraulic resistance in irrigation, but studies have shown that field-measured n values can deviate substantially from recommended values (e.g., Etedali et al., 2012). With free-draining systems, recession times depend on the surface storage volume at cutoff time and can be used to adjust the roughness coefficient. Such information is unavailable with blocked-end systems. Even with free-draining systems, volume balance results become increasingly sensitive to the roughness coefficient as the ratio of surface storage to applied volume (V_y/V_{in}) increases. In extreme cases, inadequate values of the roughness coefficient will produce an anomalous relationship for V_z versus time that is difficult to fit. However, in general, and depending on the available irrigation measurements, infiltration solutions can be developed using a range of roughness parameter values. It should be clear then that sensitivity analyses are critical when estimating infiltration without independent estimates of the roughness parameter. The application provides outputs that can be used to assess the sensitivity of surface and subsurface volumes to the roughness parameter.

Surface Volumes Determined from Flow Depth Hydrographs

This approach requires a set of depth hydrographs measured at more or less regular distance intervals and must include hydrographs for the field boundaries (Strelkoff et al., 1999). The EVALUE component requires a minimum of five depth hydrographs. Depth and water elevation profiles are reconstructed from the depth hydrographs using linear interpolation. Plots of the profiles can be used to identify and correct anomalies in the data. Values of V_y are computed from these profiles using trapezoidal rule integration. Because the trapezoidal rule assumes that the integrand varies linearly between computational points, flow depths need to be measured at a reasonable number of points along the field, preferably evenly spaced. During advance, integration uses a shape factor (σ_y^{Tip}) that is applied to the stream tip cell. The tip cell is the region defined by two consecutive advance and flow depth meas-

urement stations [$x_{A,i\text{-}1}$, $x_{A,i}$], where the subindex i identifies the advance distance at time t_i. The σ_y^{Tip} value is calculated using the equations presented in the previous section but adapted to the interval [$x_{A,i\text{-}1}$, $x_{A,i}$]. Considering the limited accuracy of field-measured flow depths, the sensitivity of V_y calculations to erroneous values, and the limitations of the trapezoidal rule integration method, a more sophisticated approach for determining σ_y^{Tip} is not warranted.

INTEGRATION OF INFILTRATION PROFILE

Infiltration Models

A brief overview of the infiltration modeling approaches used by the software needs to be provided prior to describing the methods used to integrate the infiltration profile.

Different variations of equation 13, referred to here as the modified Kostiakov equation, are used to model infiltration as a function of opportunity time only (Bautista et al., 2009a; Bautista, 2016):

$$A_z = W_1\left(k\tau^a + b\tau\right) + W_2 c \tag{13}$$

where k [L/T^a], a [.], b [L/T], and c [L] are empirical parameters (representing the α parameters in equation 2, while W_1 and W_2 are transverse lengths [L]. The k and a parameters represent transient infiltration, b a steady-state infiltration rate, and c is a fitting parameter when representing the NRCS infiltration families or instantaneous infiltration into soil macropores otherwise.

The transverse length variables are used to represent different assumptions about the infiltration process. When modeling infiltration in borders, where infiltration is essentially one-dimensional, $W_1 = W_2 = BW$, where BW is the border width. When modeling furrow infiltration, the transverse length is used to represent three different assumptions about the infiltration process:

Case 1: $W_1 = W_2 = FS$, where FS is the furrow spacing, applies if infiltration is assumed to be independent of wetted perimeter effects and therefore of flow depth. Use of this option is justified when the resulting infiltration equation is expected to be used under a range of inflows close to the value used during the evaluation, or when there is reason to believe that infiltration rates for a particular soil are insensitive to inflow variations. Such behavior has been observed in erosive soils, as a result of sediment deposition, and in cracking soils.

Case 2: $W_1 = W_2 = W_{PNRCS}$, where W_{PNRCS} is the wetted perimeter of the NRCS infiltration model, while the parameters k, a, and c are those of the NRCS infiltration families ($b = 0$).

Case 3: $W_1 = WP_0$ and $W_2 = FS$, where WP_0 is a representative wetted perimeter computed from the average inflow rate. This method for adjusting infiltration with a wetted perimeter is nearly the same as the method used by the revised NRCS infiltration families (Walker et al., 2006) but with the difference that the time-dependent infiltration depends on the wetted perimeter, while macropore infiltration depends on the furrow spacing.

While a wetted perimeter value calculated from the inflow conditions is used to adjust the average infiltration volume per unit length with cases 2 and 3, those methods ignore the effect of water pressure and locally variable wetted perimeter on the infiltration process. Thus, these methods still represent infiltration as a function of opportunity time only at any particular distance. Use of these approaches is justified by studies that have shown that the average infiltration rate over a furrow varies linearly with wetted perimeter (Fangmeier and Ramsey, 1978).

A one-dimensional flow-depth dependent infiltration model, applicable to border and basin irrigation, is the Green-Ampt (GA) equation (Green and Ampt, 1911). That equation can be formulated to account for variable flow depth as follows (Warrick et al., 2005):

$$z = z_0 + K_s\left(t - t_0\right) + \Delta\theta\Delta h \cdot \ln\left(\frac{z + \Delta\theta\Delta h}{z_0 + \Delta\theta\Delta h}\right) \tag{14}$$

where z is the infiltrated depth [L^3/L^2], z_0 is the infiltrated depth at time t_0, $\Delta\theta$ is the difference between the saturated (θ_s) and initial (θ_0) water content, Δh is the difference between the water pressure at the soil surface (h, expressed as a depth) and the wetting front pressure head (h_f, a negative quantity, expressed as a depth), and K_s is the saturated hydraulic conductivity [L/T]. Clemmens and Bautista (2009) noted that the Green-Ampt model often fails to model field-measured data during the early stages of the process, likely due to the effect of macropore flow. Hence, those authors suggested adding an instantaneous infiltration component (c_{GA}), as in equation 13, to empirically account for macropore infiltration. WinSRFR 5 also uses the Richards equation to represent one-dimensional infiltration, but the EVALUE component does not support the estimation of those parameters.

Warrick et al. (2007) proposed an approximate furrow infiltration model, which can be written as:

$$A_z = zWP + \frac{\gamma S_0^2 t}{\Delta\theta} \tag{15}$$

This equation expresses two-dimensional infiltration as the sum of a one-dimensional infiltration component (represented by the product of z and the wetted perimeter) and a second component representing the lateral flow of water, whose contribution increases linearly with time. The second term depends on the soil sorptivity (S_0) and an empirical parameter (γ), which is soil dependent and has a value close to 1.0. WinSRFR implements this model, modified to account for variable flow depth effects (Bautista et al., 2016), with z calculated with the Green-Ampt formula and S_0 expressed as a function of the Green-Ampt parameters (Warrick et al., 2007). Macropore infiltration is accounted for empirically. This model is identified in the software as the Warrick-Green-Ampt (WGA) model.

WinSRFR also offers a flow-depth dependent version of the modified Kostiakov equation for furrow infiltration calculations. It is identified in the software as the modified Kostiakov model, with local wetted perimeter. Perea et al. (2003) and Bautista (2016) provided computational details of this formulation and discussed its capabilities in relation to the two-dimensional Richards and WGA models, respectively.

Integration of Infiltration Profile

Numerical integration can be used to approximately solve equation 2 with either opportunity time only or flow-depth dependent infiltration models. In the latter case, numerical integration is the only method that can be used. In the former case, numerical integration is the preferred approach, but it is only used if allowed by the available data and hydraulic conditions. As will be discussed below, analytical solutions to equation 2 are prone to systematic errors under some conditions.

Numerical approximation can only be applied if the available data can be used to determine A_z at more or less regular distance intervals x_k, including the wetted field boundaries. As with surface volume measurements, at least five measurement stations are required, preferably evenly spaced. Clearly, the number of recommended measurement points depends on field length and other field considerations and needs to be determined case-by-case. The integration is performed again using the trapezoidal rule method, with a shape factor (σ_z^{tip}) applied to the tip cell:

$$\sigma_z^{tip} = \frac{1}{1+a} \tag{16}$$

where a is the exponent of equation 13.

Analytical solutions to equation 2 have been developed only for cases where A_z is a function of opportunity time only. The solution requires the Lewis and Milne (1938) variable transformation:

$$V_z^*(t) = \int_0^{t_A} A_z(t - t_x)\frac{dx}{dt_x}dt_x \tag{17}$$

where t_A is the advance time to a distance x, which can be no greater than t_L, the final advance distance, and dx/dt_x is the stream advance rate. Solutions have been found for power law infiltration models by representing advance with a power law relationship (Philip and Farrell, 1964):

$$x_A = pt^r \tag{18}$$

where the parameters p [L/T^r] and r [.] are determined from advance distance-time measurements. If more than two data pairs are available, these parameters are calculated by the software using non-linear regression.

An expression for V_z^* as a function of the opportunity time at the upstream end of the field (τ_0), the stream length, and subsurface shape factors RZ_1 and RZ_2 is obtained by combining the previous two expressions with equation 13:

$$V_z^* = V_z^{*pi} = W_1\left(RZ_1 k\tau^a + RZ_2 b\tau\right)x_A + W_2 c x_A \tag{19}$$

where the notation V_z^{*pi} is used to identify predicted infiltration values computed with the power law integral. The shape factor RZ_1 [.] depends on the exponents a and r, while RZ_2 [.] depends on r only. Different shape factors apply for advance and post-advance calculations (Strelkoff et al., 2009).

Equation 19, or variants of that equation, have been used by numerous authors (e.g., Elliott and Walker, 1982; Scaloppi et al., 1995; Gillies and Smith, 2005). It is reasonably accurate in comparison with unsteady simulation results when the measured advance curve is moderately non-linear, but less accurate when the flow exhibits strong deceleration (Bautista et al., 2012b). The accuracy of equation 19 can be assessed by comparing the following ratios for every volume balance calculation time:

$$\sigma_z^{*pi}(t_i) = \frac{V_z^{*pi}}{A_{z0}^{*pi} x_A} \tag{20}$$

$$\sigma_z^{sim}(t_i) = \frac{V_z^{sim}}{A_{z0}^{sim} x_A^{sim}} \tag{21}$$

Equation 20 is a shape factor that relates the average infiltration area implied by equation 19 to the upstream infiltration area (A_{z0}). Equation 21 is a related shape factor that is computed from simulation results with the estimated infiltration function. The superscript *sim* in this expression denotes the use of simulation results. (Note that at any time t_i, $A_{z0}^{pi} = A_{z0}^{sim}$ because they are computed using the same infiltration parameters). The σ_z^{pi} value is always a decreasing function of x_A, while σ_z^{sim} eventually increases when the flow is decelerating rapidly (Bautista et al., 2012b). The EVALUE component computes and displays these shape factors and, as with the calculation of V_y, can use the unsteady simulation results to improve the calculation of V_z^{*pi}, specifically by feeding back the shape factors of equation 21 into 20 and using the resulting expression to solve for V_z^{*pi}.

ESTIMATION OF INFILTRATION FUNCTION

The basic estimation process consists of selecting an infiltration model and determining the model parameters with equation 3. The analysis is subject to the limitations of the volume balance calculations and of the selected modeling approach. Hence, the estimated function needs to be validated and adjustments need to be made iteratively if problems are identified. With borders, the infiltration model is defined by the selected infiltration equation only. With furrows, the infiltration model is defined by the approach used to model the wetted perimeter effect in combination with the selected infiltration equation. The wetted perimeter option has to be selected first and corresponds to one of the cases 1 through 3 described in the previous section. Selection of an infiltration equation for a particular field depends on the particular characteristics of the infiltration process. The Kostiakov equation (where $b = c = 0$) may fit the field-measured data under some conditions, but this simple equation may misrepresent infiltration in soils that exhibit a well-defined steady infiltration rate or substantial macropore flow.

The search for parameters that minimize equation 3 is conducted manually, with the aid of a graphical display. Use of an optimization procedure was investigated but not adopted at this time because of potential convergence problems. The parameter search generally is easy, but it can be challenging when V_z varies erratically as a function of time.

The validation process consists of an unsteady simula-

tion with the estimated function. Validation outputs include a summary of volume balance results and a comparison of pertinent measurements and simulation results, using tabular and graphical results. Depending on the available data, the analysis also compares the final field-measured and simulated volume balance and computes pertinent hydraulic performance indicators (distribution uniformity of the low quarter, runoff fraction, deep percolation fraction, application efficiency, adequacy of the low quarter, etc.).

Several components of the analysis need to be investigated when simulation results fail to adequately reproduce the available measurements. One is the magnitude of the volume balance errors (eq. 12) reported by the application. When the analysis involves estimated surface volumes, errors are associated with inadequate estimates for the parameter β of equation 5. As was previously explained, those estimates can be refined by feeding back simulation results to the volume balance calculations. When using measured volumes, volume balance errors can be related to inadequate estimates for the hydraulic resistance parameter. Procedures provided by the application to estimate the roughness parameter from measured depth hydrographs are described below. Inaccuracies associated with the integration of the infiltration profile with equation 19 were discussed earlier. Those problems can be detected by inspecting the shape factors σ_z^{pi} and σ_z^{sim}, which are reported by the software. As with the surface volumes, the software provides mechanisms for improving the infiltration integral calculations by feeding back the σ_z^{pi} values computed with the current infiltration parameter estimates. Those shape factors, like the surface factors, depend more strongly on slope and stream length than on infiltration. Thus, errors can be substantially reduced after one iteration.

There are other sources of error that cannot be properly quantified or corrected with the available data. These include inaccuracies of the trapezoidal rule integration when using measured surface volumes, and problems caused by inaccurate measurements. If those types of errors are still suspected, the graph of V_z^* versus V_z can still be used to guide the adjustment of the infiltration parameters, even if those volumes diverge at the end of the analysis.

Estimation of infiltration in surface irrigation is hampered by the limited observability of the irrigation process, soil variability, sensitivity of the calculations to the available measurements, and modeling deficiencies (Bautista and Walker, 2010). Given these uncertainties, the analysis needs to develop a range of potential solutions and focus on understanding the general characteristics of the infiltration function rather than focusing on the parameter values alone. There is little value in refining the parameter values if the resulting function remains essentially unchanged. This also means that the sensitivity of irrigation simulation results to alternative solutions needs to be investigated as part of any estimation analysis.

Fitting the Hydraulic Roughness Parameter

Hydraulic analyses of surface irrigation systems typically use the Manning roughness equation and assume standard values for the roughness coefficient. Inaccurate estimates of this parameter can have significant implications on the estimated infiltration function. This is even true when deriving surface volumes from measured depths, although the potential error is much smaller than when using estimated surface volumes.

The hydraulic roughness coefficient is adjusted based on comparisons of measured and simulated depth hydrographs. To do this effectively, more than one measured hydrograph is needed. As with the infiltration parameters, the adjustment is done manually, with the assistance of a graphical tool and goodness-of-fit indicators. Fitting can be done using the Manning or Sayre-Albertson (1966) resistance equations.

In cases where the available depth hydrographs can be used for adjusting the roughness coefficient but not for volume balance calculations, infiltration estimates will depend on an initially assumed value for the resistance coefficient. Current infiltration parameter estimates derived with that initial estimate will have to be updated after adjusting the roughness parameter. This sequence of adjustments may need to be repeated until a reasonable fit is achieved for all the available measurements.

Estimation of Parameters for Depth-Dependent Infiltration Models

In principle, the only difference between setting up an estimation problem with a depth-dependent infiltration model and a model dependent on opportunity time only is that the former always requires depth hydrographs to compute A_z. This implies that measured depth hydrographs are always needed, covering the entire length of the stream, and measured at reasonable distance intervals. A procedure was developed for the estimation of depth-dependent infiltration parameters applicable to cases where a full set of measured depth hydrographs are available, but also to cases where they are not.

The proposed procedure takes advantage of the fact that solutions to the inverse problem of surface irrigation are not unique, i.e., different infiltration functions can approximate the measured surface flow variables with similar accuracy while predicting different final distributions of infiltrated water (Bautista, 2016). Computational results will be presented below in support of this statement. The estimation proceeds in two steps.

In the first step, the field data are used to estimate an infiltration function dependent on opportunity time only. The procedures described earlier are used for this step. An estimate for the roughness parameter is also obtained during this stage, if allowed by the available data. The objective is to fit the predicted flow variables (advance and recession times, runoff, and flow depths if available) to the measured values as closely as possible. In the second step, the depth hydrographs simulated using the infiltration (and roughness) parameters developed in step 1 are used as inputs to the depth-dependent infiltration models. Because A_z values can be calculated at any point (x, t) in the computational grid generated by the simulation, V_z can be computed at the available volume balance calculation distances and times using trapezoidal rule integration. As in step 1, V_z^* values are matched to the volume balance results (V_z) by adjusting

the infiltration model parameters. Because the parameters of the Green-Ampt and Warrick-Green-Ampt models have physical meaning, they need to be adjusted considering realistic values.

COMPUTATIONAL TESTS

The following tests illustrate the computational capabilities and limitations of the proposed procedures. Practical applications will be discussed in a separate article. For these tests, simulated irrigation events provided the irrigation measurements. In the following discussion, those data are identified as the "observations" or "measurements" to distinguish them from the simulation results derived with the estimated infiltration function. The simulations were conducted assuming uniform field conditions and with infiltration given by the either the Green-Ampt (GA) model (borders) or the Warrick-Green-Ampt (WGA) model (furrows). Geometry, infiltration, hydraulic resistance, and boundary condition information for the simulated irrigations are given in table 1. The same Green-Ampt parameters were used for all simulations. Table 1 also provides two performance indicators that are relevant to the discussion: the final advance time t_L and the ratio V_y/V_{in}, which was calculated at t_L for scenarios 2 through 5 and at cutoff time t_{co} for scenario 1 because in that case $t_{co} < t_L$. Infiltration function estimates were developed with infiltration given by the modified Kostiakov equation (with $c = 0$ cm). With the furrow tests, infiltration estimates were developed assuming no wetted perimeter effects (case 1).

TEST 1

A consideration when using flow depth measurements to determine surface volume is the spacing between depth measurement stations. This spacing determines the length of the computational cells used to numerically integrate both the surface and subsurface volumes. This part of the analysis examines the integration errors as a function of stream length and of the spacing between measurement stations. The test uses the data from irrigation 1 (a basin system). Three evaluation scenarios were examined based on flow depths given at distance intervals (Δx) of 12.5, 25, and 50 m (representing 17, 9, and 5 evenly spaced measurement stations, respectively). Other inputs included advance and recession times, and geometry and boundary condition data. In this test, cutoff precedes the final advance time (table 1), recession begins shortly thereafter, and all water infiltrates 100 min later. This essentially limits the calculation of volume balance to the available advance and recession times. For each scenario, all available advance times and the recession times at 0, 50, and 150 m were selected for the analysis. Because the ratio V_y/V_{in} is very large for this example (table 1), V_z estimates (eq. 1) are very sensitive to estimates of V_y.

In the first part of the analysis, equation 12 was used to quantify the relative error of the volume balance V_y in comparison with the observed values V_v^{sim}. Evidently, in practical cases, the actual surface volumes would be unknown. The second part of the analysis examined the associated V_z^* errors. Instead of comparing V_z^* values with observed values, V_z^* values computed at $\Delta x = 25$ m and $\Delta x = 50$ m were contrasted with results computed at $\Delta x = 12.5$ m using a common infiltration function. This approach was used to eliminate the effect of V_y integration errors on the analysis. The common function was estimated using $\Delta x = 12.5$ m, which in principle yields the most accurate result. Relative infiltration integration errors were computed as:

$$E_{Vz*}(\%) = \frac{V_z^n - V_z^{17}}{V_{in}} \times 100 \tag{22}$$

where the superscript is used to identify the number of stations (5 or 9) used in the calculations.

Figure 1 shows E_{Vy} for each spacing scenario as a function of the volume balance calculation time. The labels inside the graph identify the associated advance distances. At short advance distances, and therefore short volume balance calculation times, errors are dominated by the tip cell shape factor. Because the application generated a fairly accurate shape factor for this example, it was manually set at the conventional 0.77 value to better illustrate how this effect gradually disappears as the stream elongates. Better accuracy is achieved as more flow depth measurement stations are used to calculate V_y, as would be expected. However, in all cases, errors are close to 1% after the water reaches 100 m and continue to decrease during the post-advance phase.

Errors associated with the integration of the infiltrated volume (fig. 2) exhibited similar patterns as the surface volume, which is again related to the influence of the subsurface tip cell shape factor. Nearly the same results were computed with nine stations as with 17 stations. While calculations with five stations produced absolute relative er-

Table 1. Simulated irrigations used for computational tests.

	Irrigation 1	Irrigation 2	Irrigation 3	Irrigation 4	Irrigation 5
System type	Basin	Furrow	Border	Furrow	Furrow
Length	200 m	200 m	200 m	200 m	200 m
Slope (m m^{-1})	0.0005	0.0005	0.0035	0.005	0.0005
Furrow cross-section	Bottom width (BW) = 0.2 m, side slope (SS) = 1 m m^{-1}, and furrow spacing (FS) = 1 m				
Downstream boundary condition	Blocked	Blocked	Open	Open	Blocked
Infiltration parameters (GA and WGA models)	$\theta_s = 0.42$ cm cm^{-1}, $\theta_0 = 0.18$ cm cm^{-1}, $h_f = -30$ cm, and $K_s = 1.5$ cm h^{-1}				
Hydraulic resistance	Manning $n = 0.125$	Manning $n = 0.04$	Manning $n = 0.125$	Manning $n = 0.04$	Sayre-Albertson $\chi = 0.004$ m
Inflow rate (Q_{in}) and cutoff time (T_{co})	$Q_{in} = 3$ L s^{-1} m^{-1}, $T_{co} = 120$ min	$Q_{in} = 1$ L s^{-1}, $T_{co} = 360$ min	$Q_{in} = 2$ L s^{-1} m^{-1}, $T_{co} = 270$ min	$Q_{in} = 1$ L s^{-1}, $T_{co} = 480$ min	$Q_{in} = 1.25$ L s^{-1}, $T_{co} = 270$ min
Performance measures					
Final advance time (t_L, min)	151.9	247.5	193.5	132.3	108.3
V_y/V_{in}	0.47	0.11	0.24	0.11	0.21

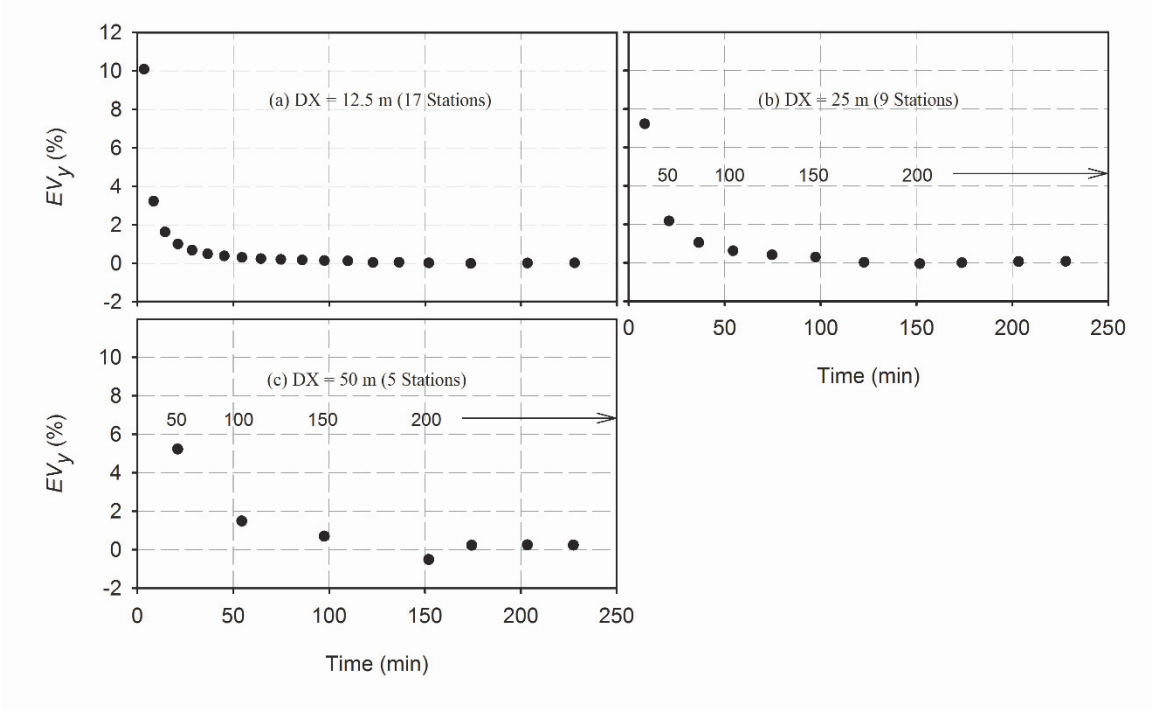

Figure 1. Test 1: Relative errors in the determination of surface volume from measured flow depths as a function of time and the distance between measurement stations: (a) Δx = 12.5 m, (b) Δx = 25 m, and (c) Δx = 50 m.

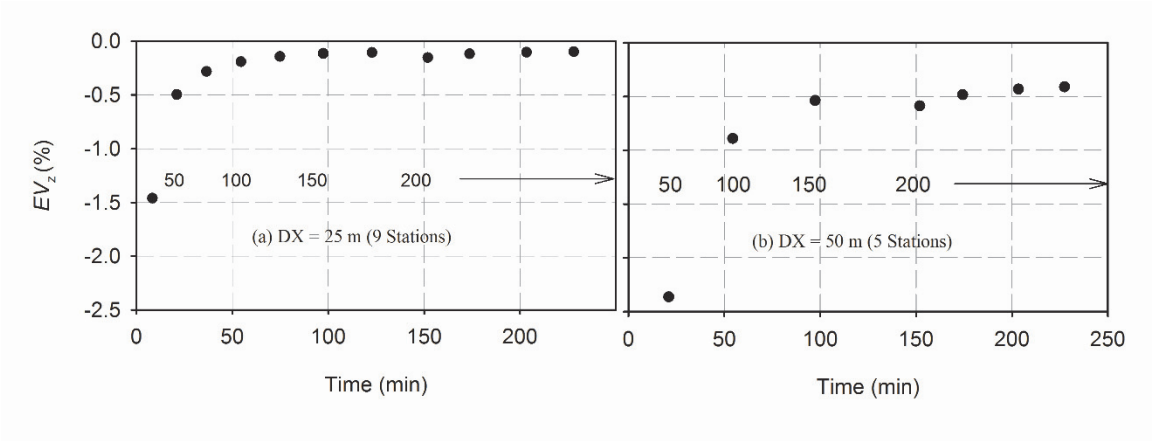

Figure 2. Test 1: Errors in the integration of the infiltration volume calculated for (a) 25 m and (b) 50 m long computational cells in comparison with the solution computed at 12.5 m intervals.

rors of less than 1% after 100 m, those errors were about 4 times as large as with nine stations.

While these results are for a single example derived from simulated data with perfect measurements, they show that it is possible to obtain reasonable volume balance results with relatively widely spaced stations, but mostly if the available information can be used to calculate volume balance relationships during the post-advance phase. This is because V_z (as a result of the errors in determining V_y) and V_z^* are both inaccurate when calculated from a few computational cells. In addition, users must consider the influence of erratic flow depth measurements at relatively short advance distances, which can lead to negative V_z values or to values that do not vary monotonically with time.

TEST 2

Volume balance analyses often use equation 4 to determine V_y and equation 19 to determine V_z^*. Test 2 illustrates the inaccuracies of these equations. The test uses the example identified as irrigation 2 (table 1), a low-gradient, blocked furrow. In order to force the volume balance analysis to calculate V_y with equation 4, no depth hydrographs were provided as inputs to the EVALUE component. This also forces EVALUE to calculate V_z^* with equation 19. Because V_y cannot be calculated with equation 4 during the post-advance phase with a blocked-end irrigation system, volume balance can only be calculated during the phase and at the final recession time, if the available data can be used to compute a post-irrigation volume balance. This analysis used only advance times, measured at 25 m intervals. With this irrigation, advance is very non-linear near the end of the field. As a result, the power advance law (eq. 18) fits the advance data poorly and yields a small ex-

ponent value (0.41). The test first examines the effect of equation 4 alone, by calculating V_z^* numerically, and then examines the combined effect of equations 4 and 19.

With both parts of the test, an infiltration function was estimated from the initially calculated volume balance. The shape factors generated by the simulation were then fed back to the volume calculations, and a new function was estimated. Iterations were stopped when the calculations produced only minor improvements to the volume balance errors. Three iterations were required when dealing with the errors of equation 4 alone, and four iterations were required when dealing with equations 4 and 19.

Figure 3 illustrates the initial (dotted line) and final (solid line) estimated infiltration functions for both sets of calculations. When equation 4 was used alone (fig. 3a), iterative adjustments to the surface volumes produced only small changes in the shape of the infiltration function. Two factors account for the small improvement. First is that the volume balance calculations are not very sensitive to the shape factor with this example because V_y/V_{in} is relatively small during advance (table 1). In addition, the volume balance errors of the initial iteration depend on the shape factors initially generated by the application. For this case, the initial estimate was reasonably accurate and resulted in an initial EV_y of about 2%. Initial errors can be greater under other hydraulic and soil conditions.

The differences between the initial and final solution were more substantial when using equations 4 and 19 (fig. 3b), even though the computed volume balance error was only about 4%, thus apparently not much greater than with the previous set of calculations. The limitations of the power law integral were previously explained. Figure 4 plots the shape factors σ_z^{sim} (eq. 21) and σ_z^{pi} (eq. 20) calculated during the initial iteration. The key results are the values calculated at the measured final advance time. Calculations with equation 19 and the estimated infiltration function yield $\sigma_z^{pi} \approx 0.73$, while the simulation with the same function yields $\sigma_z^{sim} \approx 0.84$. The ratio of these factors multiplied by 200 m (the actual advance distance at 247.5 min) is the advance distance predicted by the simulation (173 m). With the solution calculated in the first iteration, the stream never reaches the end of the field.

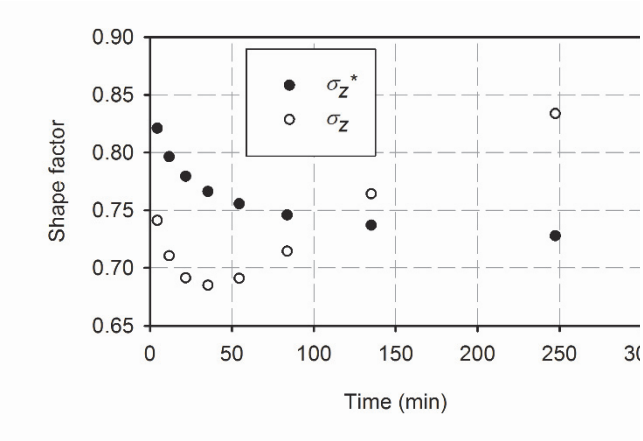

Figure 4. Test 2: Infiltration shape factors implied by the power law integral for test 2 in comparison with the shape factors implied by unsteady simulation results.

TEST 3

This test examines the spatial and temporal variation of surface flow depths when infiltration is modeled with a depth-dependent infiltration model and with a model that depends on opportunity time only. The proposed procedure for estimating the parameters of depth-dependent infiltration models relies on being able to predict the same surface flow with both approaches. This is akin to assuming that interactions between the infiltration and hydraulic resistance processes are negligible. Clearly, strong interaction between the infiltration and hydraulic resistance processes would hamper our ability to estimate the corresponding parameters with either volume balance or simulation/optimization methods.

The first part of this analysis uses scenarios 1 through 4. In all cases, parameters of the modified Kostiakov model were estimated using flow depths, advance and recession times, captured at 25 m intervals; runoff rate was also used with the free-draining systems. These tests assume that hydraulic resistance is described by the Manning equation, as in the original simulation. Hence, the estimated functions were validated with Manning n set at the known value of the original simulation (0.125 for the borders and 0.04 for

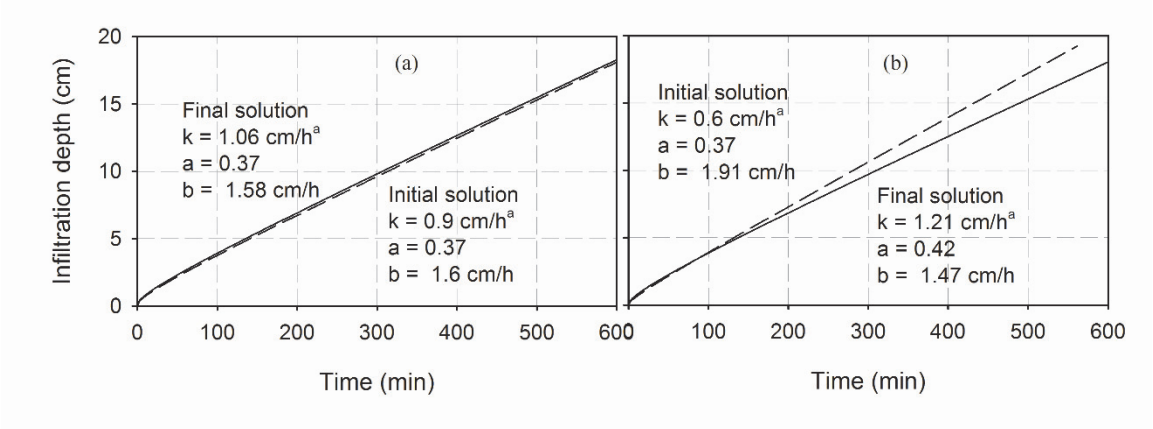

Figure 3. Test 2: Impact of errors in the calculation of V_y with equation 4 and V_z^* with equation 19 on the estimated infiltration function showing initial and final results: (a) analysis conducted with equation 4 only and (b) analysis conducted with equations 4 and 19.

the furrows). Agreement between the simulated and observed depth hydrographs at each measurement station was evaluated using the percent bias (PBIAS) indicator (Gupta et al., 1999). This indicator measures the tendency of a model to over- or under-predict an observed time series, with negative values indicating overprediction.

Figure 5 summarizes the PBIAS indicators computed for each scenario. Each point in the plot represents a flow depth measurement station. These results confirm that nearly the same surface flow depths can be predicted assuming that infiltration depends on the local variation in flow depth, as when assuming that infiltration is a function of opportunity time only. This is particularly true with the graded systems. The largest differences, in absolute magnitude, were computed with the low-gradient blocked furrow system. These results are attributed to small changes in the distribution of infiltrated water along the field, which translated into a slightly larger accumulation of surface water at the downstream end of the field. Because that end of the field is under the effect of backwater, the additional surface volume necessarily increases the flow depth. This suggests that when estimating the roughness parameter in blocked systems, users should expect potentially large errors in the area affected by backwater and perhaps give greater weight to results computed farther upstream. Given this very close agreement between hydrographs, users should be able to estimate the infiltration parameters of the original simulation, or at least get very close to those values.

TEST 4

The above findings are based on the assumption that the actual hydraulic resistance is described by the empirical Manning equation. The Manning equation is widely used because of its familiarity and convenience; parameter values have been suggested for different open channel surfaces, including surface irrigation systems, which seem to be supported in practical applications, but the true nature of this process is still largely unknown. A pertinent question then is whether the proposed approach for estimating the parameters of flow-depth dependent infiltration models is still valid if the true resistance process behaves differently from the Manning model. This question can be examined by generating observations with an alternative resistance formulation, the Sayre-Albertson equation (1966):

$$C = 6.06 g^{1/2} \log_{10} \frac{R}{X} \tag{23}$$

Hence, this test uses scenario 5, with the resistance parameter X = 0.4 cm. Flow depth hydrographs obtained at 25 m intervals were provided for estimation. The estimation analysis was conducted with infiltration represented with the modified Kostiakov equation (case 1) and hydraulic resistance represented with the Manning equation. Agreement between measurements and simulation results was again evaluated by comparing the depth hydrographs using the PBIAS indicator.

Figure 6 shows the resulting modified Kostiakov infiltration function. For comparison purposes, the graph also shows the function computed for test 2, which was computed for the same soil conditions. The larger infiltration rates implied by the function estimated for this test in comparison with test 2 are consistent with the fact that they were computed for different inflow rates. The estimated infiltration parameter values are given in the graph. The estimated n value (0.03) is reasonable for a furrow system with bare soil.

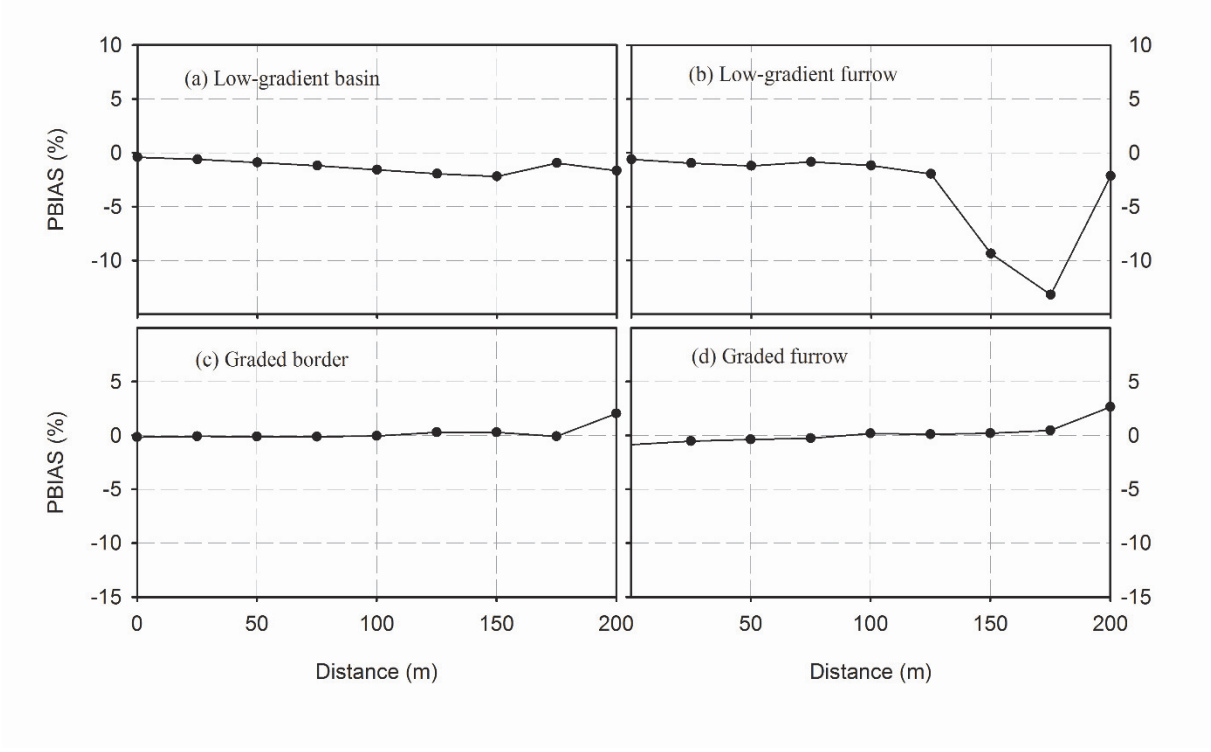

Figure 5. Test 3: Comparison of measured and simulated depth hydrographs at each measurement station.

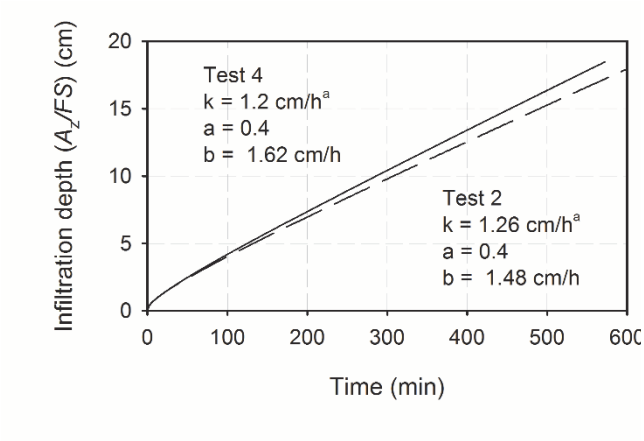

Figure 6. Test 4: Estimated infiltration function in comparison with the function estimated for test 2.

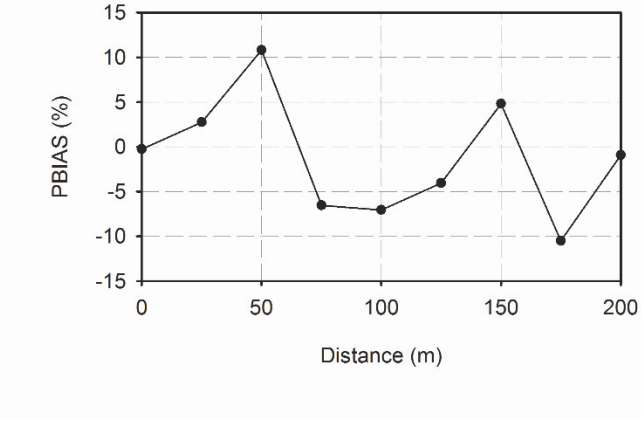

Figure 7. Test 4: Comparison of measured and simulated depth hydrographs at each measurement station.

In contrast with the results shown in figure 5, the PBIAS values computed for this test (fig. 7) are much larger and reverse their sign several times with distance. This pattern of variation cannot be explained at this time. Given these larger differences between the depth hydrographs of the original simulation and the hydrographs produced by simulation with the estimated parameters, accurate estimation of the original WGA parameters would seem less likely. The known WGA parameters and the depth hydrographs produced by the first step of the estimation were used to calculate V_z^*. Figure 8 contrasts those results with the V_z values determined by the volume balance analysis, based on the available measurements. The fact that the results are in close agreement indicates that, despite inaccuracies in modeling the hydraulic resistance process, we would still be able to solve or nearly solve for the original infiltration parameters.

CONCLUSIONS

A software component has been developed for the estimation of infiltration and hydraulic resistance parameters in surface irrigation. An objective in the development was to provide feedback to the user with respect to inaccuracies of

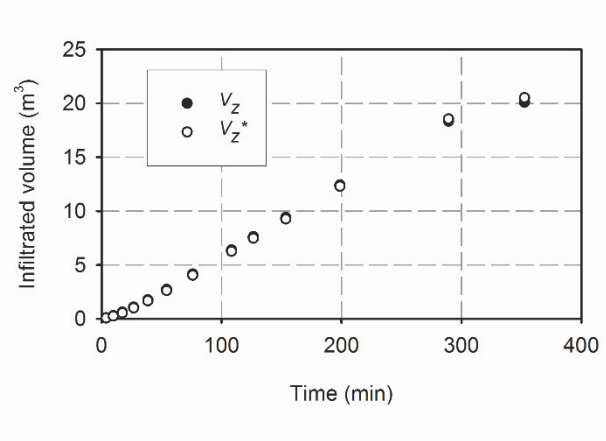

Figure 8. Comparison of measured infiltrated volumes, calculated from volume balance, with predicted values V_z^*. The predicted values were computed with the WGA model and parameters of the original simulation, but using the depth hydrographs generated with the estimated infiltration and roughness parameters.

the volume balance analysis. Results of one of the computational tests illustrated inaccuracies of the volume balance analysis under particular field conditions but also showed how those errors can be corrected to improve the reliability of results. Another objective was to enable the estimation of parameters of depth-dependent infiltration formulations. To achieve this objective, a procedure was developed that first estimates an empirical infiltration, assuming that the process is dependent on opportunity time only, and then uses the resulting depth hydrographs to estimate the parameters of a depth-dependent formulation. Computational tests provided support for this assumption, even with uncertain knowledge of the hydraulic resistance process.

REFERENCES

Bautista, E. (2016). Effect of infiltration modeling approach on operational solutions for furrow irrigation. *J. Irrig. Drain. Eng., 142*(12). https://doi.org/10.1061/(ASCE)IR.1943-4774.0001090

Bautista, E., & Walker, W. R. (2010). Advances in estimation of parameters for surface irrigation modeling and management. ASABE Paper No. IRR10-9643. St. Joseph, MI: ASABE. https://doi.org/10.13031/2013.35863

Bautista, E., Clemmens, A. J., Strelkoff, T. S., & Schlegel, J. (2009a). Modern analysis of surface irrigation systems with WinSRFR. *Agric. Water Mgmt., 96*(7), 1146-1154. https://doi.org/10.1016/j.agwat.2009.03.007

Bautista, E., Strelkoff, T., & Clemmens, A. J. (2012a). Improved surface volume estimates for surface irrigation volume balance calculations. *J. Irrig. Drain. Eng., 138*(8), 715-726. https://doi.org/10.1061/(ASCE)IR.1943-4774.0000461

Bautista, E., Strelkoff, T., & Clemmens, A. J. (2012b). Errors in infiltration volume calculations in volume balance models. *J. Irrig. Drain. Eng., 138*(8), 727-735. https://doi.org/10.1061/(ASCE)IR.1943-4774.0000462

Bautista, E., Warrick, A. W., Schlegel, J. L., Thorp, K. R., & Hunsaker. D., J. (2016). Approximate furrow infiltration model for time-variable ponding depth. *J. Irrig. Drain. Eng., 142*(11). https://doi.org/10.1061/(ASCE)IR.1943-4774.0001057

Clemmens, A. J., & Bautista, E. (2009). Toward physically based estimation of surface irrigation infiltration. *J. Irrig. Drain. Eng., 135*(5), 588-596. https://doi.org/10.1061/(ASCE)IR.1943-

4774.0000092
Elliott, R. L., & Walker, W. R. (1982). Field evaluation of furrow infiltration and advance functions. *Trans. ASAE, 25*(2), 396-400. https://doi.org/10.13031/2013.33542
Etedali, H. R., Liaghat, A., & Abbasi, F. (2012). Evaluation of the EVALUE model for estimating Manning's roughness in furrow irrigation. *Irrig. Drain., 61*(3), 410-415. https://doi.org/10.1002/ird.650
Fangmeier, D. D., & Ramsey, M. K. (1978). Intake characteristics of irrigation furrows. *Trans. ASAE, 21*(4), 696-700. https://doi.org/10.13031/2013.35370
Gillies, M. H., & Smith, R. J. (2005). Infiltration parameters from surface irrigation advance and runoff data. *Irrig. Sci., 24*(1), 25-35. https://doi.org/10.1007/s00271-005-0004-x
Gillies, M. H., Smith, R. J., & Raine, S. R. (2007). Accounting for temporal inflow variation in the inverse solution for infiltration in surface irrigation. *Irrig. Sci., 25*(2), 87-97. https://doi.org/10.1007/s00271-006-0037-9
Green, W. H., & Ampt, G. A. (1911). Studies on soil phyics. *J. Agric. Sci., 4*(1), 1-24.
Gupta, H. V., Sorooshian, S., & Yapo, P. O. (1999). Status of automatic calibration for hydrologic models: Comparison with multilevel expert calibration. *J. Hydrol. Eng., 4*(2), 135-143. https://doi.org/10.1061/(ASCE)1084-0699(1999)4:2(135)
Katopodes, N. D. (1990). Observability of surface irrigation advance. *J. Irrig. Drain. Eng., 116*(5), 656-675. https://doi.org/10.1061/(ASCE)0733-9437(1990)116:5(656)
Lewis, M. R., & Milne, W. E. (1938). Analysis of border irrigation. *Agric. Eng., 19*(6), 262-272.
Manning, R. (1889). On the flow of water in open channels and pipes. *Trans. Inst. Civil Eng. Ireland, 20*, 161-207.
Merriam, J. L., & Keller, J. (1978). Farm irrigation system evaluation: A guide for management. Logan, UT: Utah State University, Department of Agricultural and Irrigation Engineering.
Perea, H., Strelkoff, T. S., Simunek, J., Bautista, E., & Clemmens, A. J. (2003). Unsteady furrow infiltration in the light of the Richards equation. *Proc. 2nd Intl. Conf. on Irrigation and Drainage* (pp. 625-636). Denver, CO: U.S. Committee of Irrigation and Drainage.
Philip, J. R., & Farrell, D. A. (1964). General solution of the infiltration-advance problem in irrigation hydraulics. *J. Geophys. Res., 69*(4), 621-631. https://doi.org/10.1029/JZ069i004p00621
Sayre, W. W., & Albertson, M. L. (1966). Roughness spacing in rigid open channel. *J. Hydraul. Div. ASCE, 87*(3), 121-150.
Scaloppi, E. J., Merkley, G. P., & Willardson, L. S. (1995). Intake parameters from advance and wetting phases of surface irrigation. *J. Irrig. Drain. Eng., 121*(1), 57-70. https://doi.org/10.1061/(ASCE)0733-9437(1995)121:1(57)
Strelkoff, T. S., Clemmens, A. J., & Bautista, E. (2009). Estimation of soil and crop hydraulic properties. *J. Irrig. Drain. Eng., 135*(5), 537-555. https://doi.org/10.1061/(ASCE)IR.1943-4774.0000088
Strelkoff, T. S., Clemmens, A. J., El-Ansary, M., & Awad, M. (1999). Surface-irrigation evaluation models: Application to level basins in Egypt. *Trans. ASAE, 42*(4), 1027-1036. https://doi.org/10.13031/2013.13250
USDA-SCS. (1984). Chapter 5, Section 15: Furrow irrigation. In *National engineering handbook*. Washington, DC: USDA Soil Conservation Service.
Valiantzas, J. D. (1993). Border advance using improved volume-balance model. *J. Irrig. Drain. Eng., 119*(6), 1006-1025. https://doi.org/10.1061/(ASCE)0733-9437(1993)119:6(1006)
Walker, W. R. (2005). Multilevel calibration of furrow infiltration and roughness. *J. Irrig. Drain. Eng., 131*(2), 129-136. https://doi.org/10.1061/(ASCE)0733-9437(2005)131:2(129)
Walker, W. R., Prestwich, C., & Spofford, T. (2006). Development of the revised USDA-NRCS intake families for surface irrigation. *Agric. Water Mgmt., 85*(1), 157-164.
Warrick, A. W., Lazarovitch, N., Furman, A., & Zerihun, D. (2007). Explicit infiltration function for furrows. *J. Irrig. Drain. Eng., 133*(4), 307-313. https://doi.org/10.1061/(ASCE)0733-9437(2007)133:4(307)
Warrick, A. W., Zerihun, D., Sanchez, C. A., & Furman, A. (2005). Infiltration under variable ponding depths of water. *J. Irrig. Drain. Eng., 131*(4), 358-363. https://doi.org/10.1061/(ASCE)0733-9437(2005)131:4(358)